High-pressure ionic and molecular phases of ammonia within density functional theory

Gareth I. G. Griffiths and R. J. Needs
Theory of Condensed Matter Group, Cavendish Laboratory, J J Thomson Avenue, Cambridge CB3 0HE, United Kingdom

Chris J. Pickard
Department of Physics and Astronomy, University College London, Gower Street, London WC1E 6BT, United Kingdom
(Received 6 February 2012; published 1 October 2012)

We have studied ammonia under pressure using density functional theory (DFT) methods. We have used four density functionals; the local density approximation (LDA) and Perdew-Burke-Ernzerhof (PBE) semilocal functionals, the PBE + G06 semilocal functional which includes an empirical dispersion correction, and the PBE0 hybrid functional, finding results in reasonable agreement with the available experimental data in each case. Using a combination of DFT and a random-structure-searching technique, we have found a molecular phase of ammonia of space group symmetry $Pa\bar{3}$ which has not been reported in experimental studies. This phase is calculated to have a region of thermodynamic stability at low pressures with each of the four density functionals. Results with both the PBE and PBE0 functionals indicate that ammonium amide ($NH_4^+NH_2^-$) proton transfer ionic solids are stable at pressures above about 100 GPa.

DOI: 10.1103/PhysRevB.86.144102 PACS number(s): 81.40.Vw, 71.15.Nc, 31.15.A−, 61.66.Fn

I. INTRODUCTION

Ammonia is an important planetary component which exists within the ice layers of Uranus and Neptune at pressures up to about 600 GPa. Ammonia forms hydrogen-bonded solids at low pressure, but the formation of ammonium amide ($NH_4^+NH_2^-$) ionic solids at pressures greater than 100 GPa was predicted in a first-principles density functional theory (DFT) study.[1] That study used the Perdew-Burke-Ernzerhof (PBE)[2] generalized gradient approximation (GGA) semilocal density functional and the local-density approximation (LDA) functional,[3] which gave similar results. DFT calculations have been very successful in describing the relative stabilities of different phases of materials. The PBE functional has been widely tested and has yielded many fine results, and it is generally considered to be a significant improvement on the LDA. PBE-DFT generally gives a good description of closed electronic shell configurations, although it does not give an accurate account of dispersion interactions. The neglect of dispersion interactions is, however, only important in determining the relative stabilities of phases at low pressures, because at high pressures the short-range repulsion is the most critical part of the interatomic potential. The accuracy of the PBE functional has, however, recently been brought into question for proton transfer phases of ammonia monohydrate, which have been predicted to be stable at high pressures.[4] PBE-DFT predicts that proton transfer phases are stable at pressures as low as 2.8 GPa,[4,5] but such phases have not been observed in experiments.[6,7] A substantial error arises in this case because the proton transfer is accompanied by too large an electronic transfer,[4] which could be a generic failure of local and semilocal density functionals. It is therefore important to investigate the description of proton transfer reactions afforded by density functionals for other systems such as compressed ammonia.

To try and obtain higher accuracy from DFT results for ammonia monohydrate than is offered by the PBE functional we performed calculations using the PBE0 hybrid density functional[8] which includes 25% exact exchange. Use of the PBE0 functional was found to increase the enthalpy of proton transfer phases of ammonia monohydrate with respect to molecular phases by about 0.6 eV per formula unit (fu), although this enthalpy difference slowly decreased over the pressure range studied of 0–12 GPa.[4] It would take an increase in the enthalpy of the predicted proton transfer phases of ammonia of only about 0.1 eV per fu to render them unstable with respect to the molecular phases[1] which, in light of the 0.6 eV per fu increase in the enthalpy of the proton transfer phases of ammonia monohydrate mentioned above,[4] is a distinct possibility. The PBE0 results of Ref. 4 were validated by comparing with coupled cluster CCSD(T) and MP2 calculations of the interaction energies between NH_3 and H_2O molecules and between NH_4^+ and OH^- ions in the gas phase. These calculations established that the errors in the PBE results arise mainly from an overestimation of the electronic charge transfer and that the error is partially corrected by using the PBE0 functional.

The structure of phase I of ammonia was determined by neutron diffraction experiments to be of $P2_13$ symmetry.[9–11] Phase I transforms into phase IV at pressures of about 4 GPa[12–14] (phases II and III being high-temperature forms). The structure of phase IV was solved by Loveday *et al.*[12] using neutron diffraction techniques and has $P2_12_12_1$ symmetry. An ordered phase V appears at about 14 GPa[13,15,16] whose structure is currently unknown, although it is believed to be similar to that of phase IV. X-ray diffraction,[13] infrared absorption,[17] Brillouin scattering,[16] and Raman scattering studies of phases of ammonia[15,18,19] have also been performed.

The *ab initio* random structure searching (AIRSS) method[20,21] has been used to study the high pressure phases of molecular solids such as ammonia,[1] ammonia monohydrate,[6,7] hydrogen,[22] carbon monoxide,[23] nitrogen,[24] and oxygen.[25] The $P2_12_12_1$ molecular phase of ammonia has been predicted to transform into a proton transfer phase of space group $Pma2$ at about 100 GPa.[1] A transition to another proton transfer phase of $P2_1/m$ symmetry was predicted at about 340 GPa, followed by a transition to a molecular phase of $Pnma$ symmetry at

TABLE I. Gas-phase proton transfer energies for NH_3 and H_2O in eV. $\Delta E(\infty)$ corresponds to infinite separation of the ionic species, while $\Delta E(2.5\ \text{Å})$ corresponds to the assumption that the interaction between the ions is described by point charges of $\pm 1e$ separated by 2.5 Å.

	Reaction	$\Delta E(\infty)$	$\Delta E(2.5\ \text{Å})$
(1)	$NH_3 + H_2O \rightarrow OH^- + NH_4^+$	8.1	2.3
(2)	$NH_3 + H_2O \rightarrow NH_2^- + H_3O^+$	10.3	4.5
(3)	$2H_2O \rightarrow OH^- + H_3O^+$	9.8	4.0
(4)	$2NH_3 \rightarrow NH_2^- + NH_4^+$	8.8	3.0

about 450 GPa. Illustrations of the $P2_1/c$, $P2_12_12_1$, $Pma2$, $P2_1/m$, and $Pnma$ structures of ammonia and details of their structures can be found in Ref. 1, and an illustration and details of the $P2_13$ structure are given in Ref. 9.

In this study we aim to determine whether the more accurate description of proton transfer energies afforded by the PBE0 functional confirms the earlier prediction of stable ionic solids in ammonia at high pressures.[1] We have also performed additional AIRSS runs at low pressures, although at high pressures we have simply used the structures found in our previous searches.[1] We have also investigated the pressure dependence of the band gaps of the molecular and ionic phases, and the sizes of the electronic charge transfers in the ionic forms.

II. PROTON TRANSFER ENERGIES

Proton transfer energies in the NH_3-H_2O system obtained from accurate gas phase data are reported in Table I. The proton transfer energies corresponding to species at infinite separation are very large. When a solid is formed the ionic species are adjacent to one another and the Coulomb energy is greatly reduced. Table I also gives the proton transfer energies reduced by the Coulomb energy recovered by considering two point charges separated by 2.5 Å, which is similar to the molecular separation in ammonia at a pressure of about 100 GPa. The differences between the four proton transfer energies are now substantial fractions of the total proton transfer energies. In addition, the proton-transfer phases of ammonia have four more nearest neighbors of the oppositely charged species than of the same species, which will further reduce the Coulomb energy from the values given in the right-hand column of Table I, which assumes only a single neighbor of opposite charge. The proton transfer energy from H_2O to NH_3 in reaction (1) is the smallest, which is consistent with the fact that this reaction is predicted by PBE-DFT studies to occur at pressures below 10 GPa. The energy for reaction (2) is large, indicating that a proton transfer from NH_3 to H_2O is highly unfavorable, which is consistent with the fact that such a reaction has not been reported in experiments or DFT studies. Reaction (3) has a large proton transfer energy, but it is believed to occur at high pressures and temperatures in the "superionic" phase of water which consists of short-lived H_2O, H_3O^+ and OH^- species.[26] This phase was found in DFT molecular dynamics simulations, and experimental evidence for it has been found at pressures of 50 GPa and temperatures of 1000 K.[27] Superionic water might exist in the core of Saturn or within Neptune.[28] The energy for reaction (4), the proton transfer between NH_3 molecules, which is the main subject of this paper, has the second lowest gas-phase proton transfer energy, which is consistent with the fact that it has been predicted to occur at low temperatures and pressures above 100 GPa.[1] A superionic phase of ammonia has also been found in molecular dynamics simulations.[26]

III. METHODS

Our DFT calculations were performed using the CASTEP[29] plane wave code and the PBE[2] and PBE0[8] exchange-correlation density functionals. We also repeated some of the calculations using the LDA functional. We have used norm-conserving pseudopotentials generated with the OPIUM software,[30] as CASTEP is not currently able to use the more accurate and efficient ultrasoft pseudopotentials[31] in conjunction with explicit exchange. A Monkhorst-Pack k-point sampling grid[32] of spacing $2\pi \times 0.07\ \text{Å}^{-1}$ was found to be sufficient for the searches, and the use of ultrasoft pseudopotentials allowed a low plane wave cutoff energy of 290 eV to be used. To obtain our final results we used a higher level of accuracy consisting of a plane wave cutoff energy of 900 eV for both the PBE and PBE0 calculations, and Brillouin zone sampling grids of spacing $2\pi \times 0.03\ \text{Å}^{-1}$ (PBE) and $2\pi \times 0.05\ \text{Å}^{-1}$ (PBE0). Calculations were also performed with the PBE functional with the Grimme semiempirical dispersion correction (G06),[33] using the higher level of accuracy described for the PBE calculations. With these settings the resulting error in the PBE enthalpy difference between the phases was determined to be less than 0.4 meV per fu. The much more computationally expensive PBE0 calculations (between two and three orders of magnitude greater than the equivalent PBE calculation for these systems) preclude geometry optimizations of all of the structures across the broad pressure range studied, and therefore some of the PBE0 calculations were performed on the relaxed PBE structures. Further details of the calculations for which a full PBE0 geometry relaxation was possible are described in Sec. V. The less dense Brillouin zone sampling grids used in the PBE0 calculations increased the errors in the enthalpy differences between phases, but we estimate that they are still smaller than 1 meV per fu.

IV. TRANSITION PRESSURES

We have recalculated the structures and enthalpy-pressure diagram (Fig. 1) using norm-conserving pseudopotentials, obtaining excellent agreement with our previous study in which ultrasoft pseudopotentials were used.[1] The highest pressure transition discussed here ($P2_1/m \rightarrow Pnma$) differs in pressure by only 15 GPa from our earlier results, while the lower transition pressures are almost identical. These results provide strong evidence for the accuracy of the pseudopotentials used in this study and in Ref. 1. The enthalpy-pressure relation calculated using the PBE0 functional and the PBE structures is shown in Fig. 2.

In our earlier PBE DFT study of ammonia we found a small region of stability for a molecular $P2_1/c$ phase between the observed phases I ($P2_13$) and IV ($P2_12_12_1$),[1] and this result was reproduced in the current study. There have, however, not been any experimental reports of an intermediate

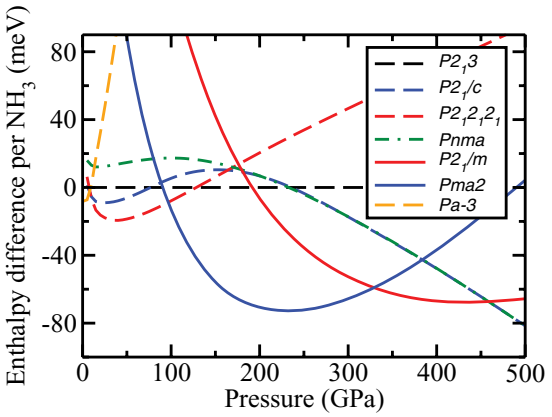

FIG. 1. (Color online) Enthalpy relative to the $P2_13$ phase as a function of pressure, calculated with the PBE semilocal functional. Solid lines correspond to ionic structures, and dashed lines to molecular structures.

phase between $P2_13$ and $P2_12_12_1$, and the predicted stability of the $P2_1/c$ phase in the PBE calculations could be an artifact of the approximate density functional. In fact our PBE0 results (Fig. 3) do not predict a region of stability for $P2_1/c$, although it is almost degenerate with the observed $P2_12_12_1$ phase at 5 GPa. The $P2_13 \rightarrow P2_12_12_1$ transition is predicted to occur at 6 GPa in PBE and 5 GPa in PBE0, which are a little larger than the observed values of about 4 GPa.[12,13,15,16] Similarly, our results with the PBE functional and G06 dispersion correction in Fig. 3 do not predict a region of thermodynamic stability for the $P2_1/c$ phase, while the $P2_13 \rightarrow P2_12_12_1$ transition pressure is underestimated; it is predicted to occur at 2 GPa. Conversely, however, calculations with the LDA functional predict a window of stability for the $P2_1/c$ phase between 3.6 and 7.8 GPa. Using the LDA functional the $P2_13 \rightarrow P2_12_12_1$ transition pressure of 4.6 GPa would be in reasonable agreement with the experimental value,

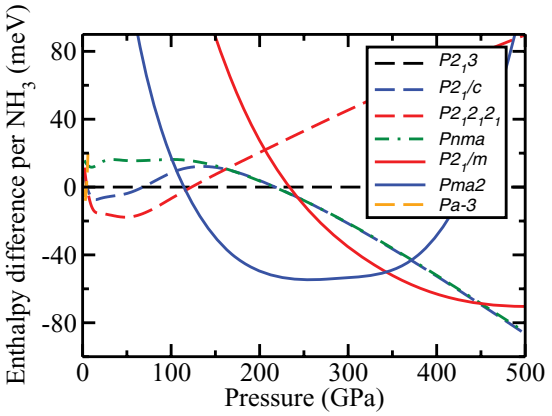

FIG. 2. (Color online) Enthalpy relative to the $P2_13$ phase as a function of pressure, calculated with the PBE0 hybrid exchange-correlation functional. Solid lines correspond to ionic structures, and dashed lines to molecular structures. The enthalpy differences between the phases were calculated using the PBE structures, with the exception of the enthalpy difference between the $P2_13$ and $Pa\bar{3}$ phases, which was calculated using structures relaxed with the PBE0 functional, as described in the main text.

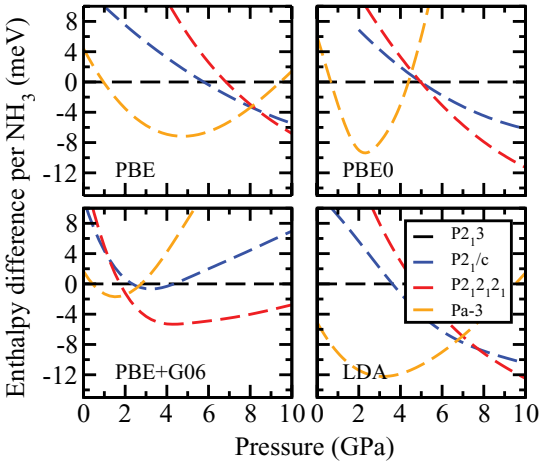

FIG. 3. (Color online) Enthalpies of the low-pressure molecular phases of ammonia, relative to the $P2_13$ phase as a function of pressure, with the PBE, PBE0, PBE + G06 and LDA functionals. The PBE0 enthalpy differences between the phases were calculated using the PBE structures, exception of the enthalpy difference between the $P2_13$ and $Pa\bar{3}$ phases, which was calculated using structures relaxed with the PBE0 functional, as described in the main text.

although at this pressure neither phase is calculated to be thermodynamically stable.

At higher pressures we find the PBE and PBE0 transition pressures to be very similar, with PBE0 giving $P2_12_12_1 \xrightarrow{116} Pma2 \xrightarrow{343} P2_1/m \xrightarrow{450} Pnma$, and PBE giving $P2_12_12_1 \xrightarrow{97} Pma2 \xrightarrow{329} P2_1/m \xrightarrow{458} Pnma$, where the numbers above the arrows give the transition pressures in GPa. There is a small difference between the PBE enthalpy-pressure curves obtained in this study and in Ref. 1 as we find that the $P2_1/c$ phase evolves continuously into the higher-symmetry $Pnma$ phase at high pressures, while in Ref. 1 the $P2_1/c$ symmetry was maintained and it did not fall into the $Pnma$ supergroup. This difference is unimportant as it occurs in a region where neither phase is thermodynamically stable.

In the $Pma2$ ionic phase, which is stable between about 110 and 340 GPa, each NH_2^- ion has 8 NH_4^+ nearest neighbors and 4 NH_2^- nearest neighbors, with N–N distances of about 2.5 Å at 100 GPa. The N–N separations for the second nearest neighbors are greater than 3.6 Å. The N atoms in $Pma2$ form a distorted face centered cubic (fcc) structure, while in $P2_12_12_1$ they form a distorted hexagonal close packed (hcp) structure.

V. *AB INITIO* RANDOM STRUCTURE SEARCHING

The AIRSS method (as described in Refs. 20 and 21) was used in its most basic guise in our original study of ammonia, in which unit cells containing 1, 2, 3, and 4 formula units (fu) of NH_3 molecules were searched.[1] Despite the exponential increase in the number of local minima with the number of atoms in a system, we have extended the search over structures up to and including 8 fu with the use of symmetry constraints, which reduce the dimensionality of the search space. We applied $n = 2$ and $n = 4$ symmetry operations to preformed NH_4 and NH_2 units placed randomly within the unit cell, to form initial structures with 4 and 8 fu, respectively. The structures were relaxed to a minimum in the enthalpy at

TABLE II. Structural parameters of $Pa\bar{3}$ at 5 GPa calculated with the PBE functional at the higher level of accuracy.

Structure	Lattice parameters (Å, °)			Atom	Atomic coordinates (Fractional)		
$Pa\bar{3}$	a = 5.847	b = 5.847	c = 5.847	N1	0.335903	0.164097	−0.164097
	$\alpha = 90$	$\beta = 90$	$\gamma = 90$	H1	0.507657	0.181437	−0.200317

10 GPa. As mentioned earlier, we only performed structure searches at low pressures, and we used the structures found in our previous searches[1] at high pressures.

Our search over structures at 10 GPa with 8 fu per unit cell revealed a different molecular structure of ammonia. The primitive unit cell contains $Z = 8$ fu, with space group symmetry $Pa\bar{3}$. The $Pa\bar{3}$ phase is calculated to be thermodynamically stable from 1 to 8 GPa within PBE, with a maximum stability of more than 7 meV per fu over the $P2_13$ phase. Using the PBE functional with the G06 dispersion correction substantially reduces the enthalpy differences between the molecular phases (as seen in Fig. 3); however, $Pa\bar{3}$ is still found to have a region of thermodynamic stability between 0.4 and 1.4 GPa. The relative enthalpy of $Pa\bar{3}$ was calculated at the higher level of accuracy discussed in Sec. III and is shown on the PBE phase diagram in Fig. 1. Changes in the relative enthalpies of a few meV per fu would make a significant difference to the relative stabilities of the low-pressure structures. However, we expect very strong cancellations of errors in the enthalpy differences between structures because all of the competitive low-pressure structures consist of hydrogen-bonded ammonia molecules and have very similar volumes. We note that each of the four density functionals tested predicts a region of stability for the $Pa\bar{3}$ structure at low pressures. Our prediction of a stable $Pa\bar{3}$ structure may therefore be robust. The structural parameters of this phase, calculated with the PBE functional, are reported in Table II, and the structure is shown in Fig. 4.

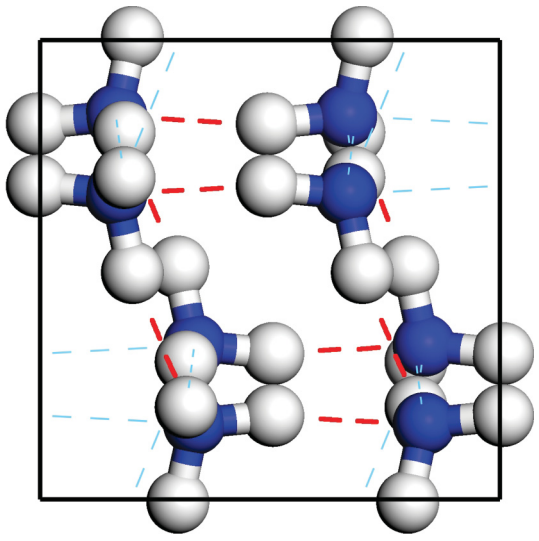

FIG. 4. (Color online) The $Pa\bar{3}$ structure at 5 GPa calculated with the PBE functional. The white spheres indicate hydrogen atoms, and the blue (dark gray) spheres indicate nitrogen atoms. Dashed lines denote hydrogen bonding; those in red (thicker) emphasize the parallelepiped of ammonia molecules in the structure. Each ammonia molecule both donates and accepts three hydrogen bonds.

Both the $P2_13$ and $Pa\bar{3}$ phases have cubic symmetry, which reduces the computational cost of the DFT calculations. For these two phases it proved computationally feasible to relax the atomic coordinates within their fixed cubic unit cells using the PBE0 functional. This was repeated for several scaled unit cell volumes, and hence by evaluating the derivative of the energy of the relaxed structures with respect to volume the enthalpy difference between these two phases was obtained over a range of pressures.

The PBE0 panel of Fig. 3 shows that $Pa\bar{3}$ is calculated to be the thermodynamically most stable phase over a substantial pressure range from 1 to 4.5 GPa, with an enthalpy of up to 10 meV per NH_3 molecule lower than the known $P2_13$ phase. A small (∼0.01 Å) contraction of the N-H bonds is observed in both $P2_13$ and $Pa\bar{3}$ upon relaxation of the PBE structures with PBE0 in a fixed unit cell. Results obtained with the LDA functional (Fig. 3, LDA panel) also show a substantial region of thermodynamic stability for the $Pa\bar{3}$ phase.

VI. ELECTRONIC STRUCTURE

A Mulliken population analysis of the molecular $P2_13$ and ionic $Pma2$ and $P2_1/m$ phases showed that the charge transfers predicted by the PBE and PBE0 functionals are almost the same. There were no significant charges on the NH_3 monomers at low or high pressures. We found charges of about $+0.5e$ on the NH_4^+ ions in $Pma2$ at ∼10 GPa, which decreased to about $+0.3e$ at 400 GPa (with the requisite negative charge on the accompanying NH_2^- ions). Similar results were found for the $P2_1/m$ ionic phase.

An isolated ammonia molecule has three energy levels. The lowest energy $1a_1$ molecular orbital derives from the nitrogen $2s$ atomic orbitals and the hydrogen $1s$ atomic orbitals. The doubly degenerate $1e$ molecular orbitals derive from the nitrogen $2p$ and hydrogen $1s$ orbitals. The highest energy $2a_1$ orbital derives from the nitrogen $2p$ orbitals and corresponds to the nonbonding lone pair. The electronic density of states (EDoS) of the $P2_13$ molecular phase at 1 GPa (Fig. 5) shows the same three distinct occupied energy regions as the isolated molecule, although they are broadened and split by the interactions between molecules. The electronic structure of $P2_13$ therefore corresponds to that of weakly interacting ammonia molecules.

The EDoS of the ionic proton transfer $Pma2$ phase at 100 GPa is shown in Fig. 6. The total occupied bandwidth of 24 eV is considerably larger than the bandwidth of 17 eV of the $P2_13$ phase at 1 GPa. The three regions apparent in the EDoS of $P2_13$ are present in $Pma2$, although they show substantial broadening and the EDoS from the two upper energy regions overlap. The EDoS of the two lower energy regions are separated by a gap of about 2 eV. The EDoS of the molecular $P2_12_12_1$ molecular phase (not shown) at 100 GPa is

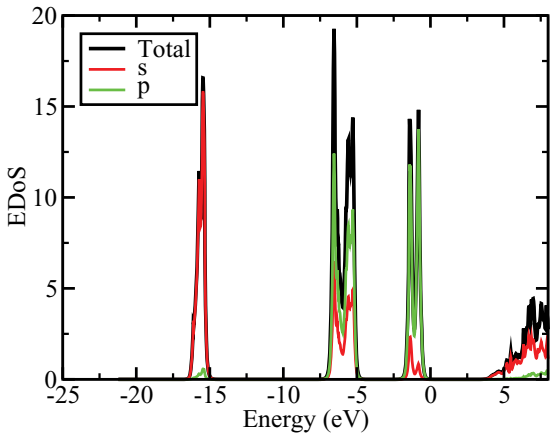

FIG. 5. (Color online) EDoS of the $P2_13$ molecular structure of phase I of ammonia at 1 GPa with the top of the valence band at zero energy. Note that the lowest energy region is almost entirely s like while the highest energy occupied region is predominantly p like.

very similar to that of $Pma2$, although the bandwidths of the two lower energy regions are a little larger in $Pma2$, signifying a larger interactions between the ions. This is consistent with the fact that the volume of $Pma2$ is 2% smaller than that of $P2_12_12_1$ at 100 GPa. The proton transfer does not therefore lead to substantial changes in the EDoS.

The minimum band gaps obtained with the LINDOS code[34] are shown in Fig. 7. The minimum band gaps of the molecular and ionic phases show similar variations with pressure, although the PBE0 gaps are roughly 2 eV larger. The gaps increase rapidly with pressure up to ∼50 GPa and decline slowly at higher pressures. The $Pa\bar{3}$ phase reported here shows a considerable reduction in the band gap with increased pressure, although above 100 GPa it is far from thermodynamic stability. At 100 GPa the $P2_12_12_1$ phase has a direct band gap at the Γ point and the $Pma2$ phase has an indirect band gap

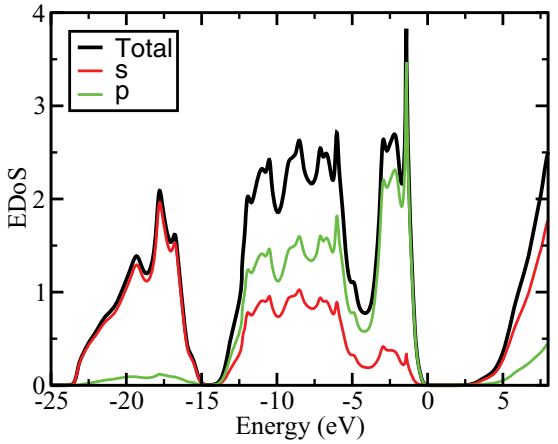

FIG. 6. (Color online) EDoS of the $Pma2$ proton transfer structure of ammonia at 100 GPa. The occupied EDoS shows the same three regions present in $P2_13$ at low pressures, but they are substantially broadened. The top of the valence band is at zero energy.

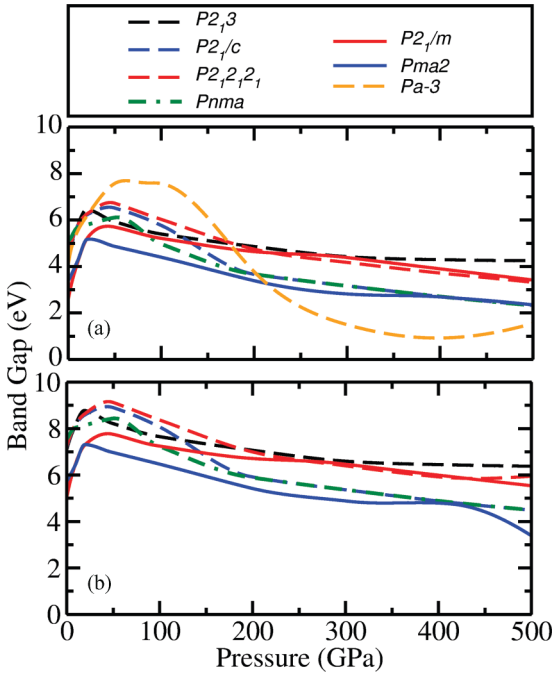

FIG. 7. (Color online) Minimum band gaps of various phases as a function of pressure with (a) the PBE functional and (b) PBE0. Solid lines correspond to ionic structures and dashed lines to molecular structures.

with the top of the valence band being at Γ while the bottom of the conduction band is at the U point.

VII. CONCLUSIONS

The tendency of H_2O, NH_3, and mixtures of them to undergo proton transfer reactions at high pressures is correlated with the sizes of the gas-phase proton transfer energies. A search over structures using the AIRSS method at 10 GPa has found a molecular $Pa\bar{3}$ phase which is very competitive at low pressures on the phase diagrams obtained with the LDA, hybrid PBE0, and PBE functional both with and without the G06 semiempirical dispersion correction. On the whole the PBE and PBE0 functionals give very similar transition pressures. The charge densities of the structures obtained with the PBE and PBE0 functionals are very similar and show only small differences in the charge transfers associated with the ionic phases. The predicted stability of ionic proton transfer phases at pressures of 100 GPa and more is therefore strongly supported by the present study. We hope that our work will motivate experiments looking for ionic phases of ammonia at high pressures and for our predicted low-pressure $Pa\bar{3}$ molecular phase.

ACKNOWLEDGMENTS

This work was supported by the Engineering and Physical Research Council (EPSRC) of the UK. Computational resources were provided by the Cambridge High Performance Computing Service. We thank Andrew Morris for help with the LINDOS code.

[1]C. J. Pickard and R. J. Needs, Nat. Mater. **7**, 775 (2008).
[2]J. P. Perdew, K. Burke, and M. Ernzerhof, Phys. Rev. Lett. **77**, 3865 (1996).
[3]J. P. Perdew and A. Zunger, Phys. Rev. B **23**, 5048 (1981).
[4]G. I. G. Griffiths, A. J. Misquitta, A. D. Fortes, C. J. Pickard, and R. J. Needs, J. Chem. Phys. **137**, 064506 (2012).
[5]A. D. Fortes, J. P. Brodholt, I. G. Wood, L. Vocadlo, and H. D. B. Jenkins, J. Chem. Phys. **115**, 7006 (2001).
[6]A. D. Fortes, E. Suard, M.-H. Lemee-Cailleau, C. J. Pickard, and R. J. Needs, J. Chem. Phys. **131**, 154503 (2009).
[7]A. D. Fortes, E. Suard, M.-H. Lemee-Cailleau, C. J. Pickard, and R. J. Needs, J. Am. Chem. Soc. **131**, 13508 (2009).
[8]C. Adamo and V. Barone, J. Chem. Phys. **110**, 6158 (1999).
[9]J. W. Reed and P. M. Harris, J. Chem. Phys. **35**, 1730 (1961).
[10]A. W. Hewat and C. Riekel, Acta Crystallogr. Sect. A **35**, 569 (1979).
[11]F. Leclercq, P. Damay, and M. Foukani, J. Chem. Phys. **102**, 4400 (1995).
[12]J. S. Loveday, R. J. Nelmes, W. G. Marshall, J. M. Besson, S. Klotz, and G. Hamel, Phys. Rev. Lett. **76**, 74 (1996).
[13]F. Datchi, S. Ninet, M. Gauthier, A. M. Saitta, B. Canny, and F. Decremps, Phys. Rev. B **73**, 174111 (2006).
[14]S. Ninet, F. Datchi, S. Klotz, G. Hamel, J. S. Loveday, and R. J. Nelmes, Phys. Rev. B **79**, 100101 (2009).
[15]M. Gauthier, Ph. Pruzan, J. C. Chervin, and J. M. Besson, Phys. Rev. B **37**, 2102 (1988).
[16]M. Gauthier, Ph. Pruzan, J. C. Chervin, and A. Polian, Solid State Commun. **68**, 149 (1988).
[17]M. Sakashita, H. Yamawaki, H. Fujihisa, and K. Aoki, Rev. High Pressure Sci. Technol. **7**, 796 (1998).
[18]T. Kume, S. Sasaki, and H. Shimizu, J. Raman Spectrosc. **32**, 383 (2001).
[19]S. Ninet, F. Datchi, A. M. Saitta, M. Lazzeri, and B. Canny, Phys. Rev. B **74**, 104101 (2006).
[20]C. J. Pickard and R. J. Needs, Phys. Rev. Lett. **97**, 045504 (2006).
[21]C. J. Pickard and R. J. Needs, J. Phys.: Condens. Matter **23**, 053201 (2011).
[22]C. J. Pickard and R. J. Needs, Nat. Phys. **3**, 473 (2007).
[23]J. Sun, D. D. Klug, C. J. Pickard, and R. J. Needs, Phys. Rev. Lett. **106**, 145502 (2011).
[24]C. J. Pickard and R. J. Needs, Phys. Rev. Lett. **102**, 125702 (2009).
[25]J. Sun, M. Martinez-Canales, D. D. Klug, C. J. Pickard, and R. J. Needs, Phys. Rev. Lett. **108**, 045503 (2012).
[26]C. Cavazzoni, G. L. Chiarotti, S. Scandolo, E. Tosatti, M. Bernasconi, and M. Parrinello, Science **283**, 44 (1999).
[27]A. F. Goncharov, N. Goldman, L. E. Fried, J. C. Crowhurst, I.-F. W. Kuo, C. J. Mundy, and J. M. Zaug, Phys. Rev. Lett. **94**, 125508 (2005).
[28]M. French, T. R. Mattsson, N. Nettelmann, and R. Redmer, Phys. Rev. B **79**, 054107 (2009).
[29]S. J. Clark, M. D. Segall, C. J. Pickard, P. J. Hasnip, M. I. J. Probert, K. Refson, and M. C. Payne, Z. Kristallogr. **220**, 567 (2005).
[30]Opium: Pseudopotential Generation Project; http://opium.sourceforge.net/ (2011).
[31]D. Vanderbilt, Phys. Rev. B **41**, 7892 (1990).
[32]H. J. Monkhorst and J. D. Pack, Phys. Rev. B **13**, 5188 (1976).
[33]S. Grimme, J. Comput. Chem. **27**, 1787 (2006).
[34]A. J. Morris and C. J. Pickard, LINDOS - version 1.3 user manual (University College London, 2011).